Molecular Therapy
Nucleic Acids
Original Article

Epigenetic Targeting of *Granulin* in Hepatoma Cells by Synthetic CRISPR dCas9 Epi-suppressors

Hong Wang,[1,3] Rui Guo,[2,3] Zhonghua Du,[1] Ling Bai,[1] Lingyu Li,[1] Jiuwei Cui,[1] Wei Li,[1] Andrew R. Hoffman,[3] and Ji-Fan Hu[1,3]

[1]Stem Cell and Cancer Center, First Affiliated Hospital, Jilin University, Changchun, China; [2]Clinical Laboratory, First Affiliated Hospital, Jilin University, Changchun, China; [3]VA Palo Alto Health Care System and Stanford University Medical School, Palo Alto, CA 94304, USA

The CRISPR-associated Cas9 system can modulate disease-causing alleles both *in vivo* and *ex vivo*, raising the possibility of therapeutic genome editing. In addition to gene targeting, epigenetic modulation by the catalytically inactive dCas9 may also be a potential form of cancer therapy. *Granulin* (*GRN*), a potent pluripotent mitogen and growth factor that promotes cancer progression by maintaining self-renewal of hepatic stem cancer cells, is upregulated in hepatoma tissues and is associated with decreased tumor survival in patients with hepatoma. We synthesized a group of dCas9 epi-suppressors to target *GRN* by tethering the C terminus of dCas9 with three epigenetic suppressor genes: DNMT3a (DNA methyltransferase), EZH2 (histone 3 lysine 27 methyltransferase), and KRAB (the Krüppel-associated box transcriptional repression domain). In conjunction with guide RNAs (gRNAs), the dCas9 epi-suppressors caused significant decreases in *GRN* mRNA abundance in Hep3B hepatoma cells. These dCas9 epi-suppressors initiated *de novo* CpG DNA methylation in the *GRN* promoter, and they produced histone codes that favor gene suppression, including decreased H3K4 methylation, increased H3K9 methylation, and enhanced HP1a binding. Epigenetic knockdown of *GRN* led to the inhibition of cell proliferation, decreased tumor sphere formation, and reduced cell invasion. These changes were achieved at least partially through the MMP/TIMP pathway. This study thus demonstrates the potential utility of using dCas9 epi-suppressors in the development of epigenetic targeting against tumors.

INTRODUCTION

Hepatocellular carcinoma (HCC) remains one of the leading causes of cancer-related death worldwide.[1,2] The preferred treatment for early stage HCC is surgical resection, but most patients are diagnosed when the disease is advanced and inoperable. Even after surgery, the prognosis of HCC is still poor, with most patients suffering recurrence and metastasis.[3] Conventional chemotherapeutics, though effective in the treatment of hepatoma, are highly toxic due to the lack of selectivity for tumor cells.[4] In spite of the rapid development of targeted therapies and immunologic checkpoint inhibitors, the disease survival in patients with HCC remains extremely low.

Granulin (*GRN*) belongs to a family of secreted glycosylated peptides cleaved from granulin-epithelin precursor (GEP). Genome-wide gene profiling has identified *GRN* as a potential therapeutic target for human cancers.[5] Recently, *GRN* has been characterized as a reliable marker for liver cancer stem cells.[6,7] As a tumor-stromal interaction factor, *GRN* plays an important role in liver metastasis by maintaining self-renewal of hepatic cancer stem cells.[8]

The CRISPR-associated Cas9 system has revolutionized the field of gene targeting.[9–11] CRISPR/Cas9 allows precise gene editing at specific genomic loci through a synthetic single-guide RNA (gRNA).[12,13] CRISPR/Cas9 can modulate disease-causing alleles both *in vivo* and *ex vivo*, raising the possibility of therapeutic genome editing.[14–17] However, the application of the Cas9 system for epigenetic targeting in cancers remains unexplored.

In this study, we explored a targeting approach that combines the Cas9 guiding system with epigenetic silencing. In this approach, three epigenetic suppressor domains, *de novo* DNA methyltransferase DNMT3a, histone 3 K27 methyltransferase EZH2, and heterochromatin-binding suppressor KRAB, were linked to the C terminus of the catalytically inactive dCas9. Using this epigenetic targeting, we examined the oncogenic role of *GRN* in hepatoma Hep3B cells. The mechanisms underlying epigenetic targeting of *GRN* in hepatoma cells were also examined.

RESULTS

Development of CRISPR dCas9 as an Epigenetic Targeting Therapy

To target *GRN* epigenetically in hepatoma, we modified the CRISPR/Cas9 system by tethering it with three epi-suppressors: DNMT3a

Received 11 April 2017; accepted 3 January 2018;
https://doi.org/10.1016/j.omtn.2018.01.002.

Correspondence: Ji-Fan Hu, MD, PhD, VA Palo Alto Health Care System, Palo Alto, CA 94304, USA.
E-mail: jifan@stanford.edu; jifanu@126.com
Correspondence: Wei Li, MD, Stem Cell and Cancer Center, First Affiliated Hospital, Jilin University, Changchun, China.
E-mail: drweili@yahoo.com
Correspondence: Jiuwei Cui, Cancer Center, First Hospital, Jilin University, 71 Xinmin Street, Changchun 130021, China.
E-mail: cuijiuwei@jlu.edu.cn
Correspondence: Andrew R. Hoffman, MD, Medical Service, Stanford University and VA Palo Alto Health Care System, Palo Alto, CA 94304, USA.
E-mail: arhoffman@stanford.edu

(*de novo* DNA methyltransferase), EZH2 (histone 3 K27 methyltransferase), and KRAB (heterochromatin binding suppressor) (Figure S1; Tables S1–S3, construct and gRNA sequences). To avoid genomic DNA breaks, a catalytically deactivated Cas9 variant (dCas9) was used to guide epigenetic targeting. This dCas9 variant is defective in DNA cleavage but maintains the ability to bind to the gRNA-guided gene target.[18,19] The binding specificity is determined by both gRNA-DNA base pairing and by a short DNA motif (protospacer adjacent motif [PAM] sequence: NGG) juxtaposed to the DNA complementary region.[20–24] In our epigenetic targeting system, the dCas9 protein bound to the target gene promoter, while the epi-suppressors silenced the activity of the target gene (Figure 1A).

We first conducted a proof-of-concept study for this approach in a cytomegalovirus (CMV) promoter-luciferase reporter system, where the CMV promoter was used to drive the luciferase reporter gene (Figure 1B). Presumably, the dCas9-epigenetic suppressors would introduce epigenetic inhibition in the CMV promoter. When the CMV promoter was epigenetically silenced, luciferase would be inhibited. We designed five gRNAs from various locations in the CMV promoter sequence (Figure S2; Table S1). The reporter vector, dCas9-suppressor vectors, and gRNA vectors were co-transfected into 293T cells. By measuring luciferase activity, we found that the potency of the dCas9 epi-suppressors was closely related to the location of the gRNA-binding sites in the promoter (Figure 1C). For example, gRNAs 1 and 2, which were located relatively far away from the transcription initiation site, did not produce significant suppression of the luciferase activity. In contrast, gRNAs 4 and 5, which were proximal to the initiation site, exhibited the maximum inhibition of the reporter gene. This pattern was observed for all three epi-suppressors (dCas9-DNMT3a, dCas9-EZH2, and dCas9-KRAB). Among the three epigenetic suppressors tested, the heterochromatin-binding suppressor dCas9-KRAB showed the best inhibition, particularly when a mixture of gRNAs (1–5) was used.

CRISPR interference has been reported to prevent transcription by steric blockage of the RNA polymerase complex.[18,25] We also observed significant inhibition of the CMV promoter activity by dCas9-gRNAs without epi-suppressors. However, greater inhibitory activity was observed in the dCas9-epi-suppressor construct groups (dCas9-DNMT3a, dCas9-EZH2, and dCas9-KRAB) than in the dCas9 group that lacked the epi-suppressors (Figure 1D). The controls, including mock-transfected cells without dCas9 (vector) or untargeted dCas9 (dCas9-gCT), had little effect on the activity of the reporter gene.

We further validated the role of the dCas9 epi-suppressors in a second reporter system, where the CMV promoter drove the copGFP gene (Figure 1E). When the mixture of gRNAs (1–5) was used for targeting, we found that the potency of epi-suppressors was KRAB > EZH2 > DNMT3a (Figure 1F). These data suggest that the heterochromatin-binding factor dCas9-KRAB yielded the best inhibition of the target gene.

Epigenetic Targeting of Oncogenic GRN in Hepatoma

GRN is a putative biomarker of hepatic cancer stem cells. To define its role in hepatoma, we first examined its expression in normal control and hepatoma patients using the dataset from the The Cancer Genome Atlas (TCGA) database of the National Cancer Institute. *GRN* was overexpressed in hepatoma as compared with normal liver (Figure 2A). When the hepatoma samples were classified based on the gene copy number variations, *GRN* was significantly upregulated in the group with *GRN* gain and amplification (Figure 2B). The hepatoma patients were then divided into high and low groups based on *GRN* expression (Figure 2C). The patients with high *GRN* expression had significantly lower survival than those with low *GRN* expression (Figure 2D).

We then used the same dCas9-epi-suppressor methodology to target the endogenous *GRN* gene in hepatoma cells. The human *GRN* promoter has been well characterized (Figure S3A),[26] and its activity is associated with epigenetic modifications.[27–29] We designed four gRNAs complementary to the *GRN* promoter (Figure 2E; Figures S3B and S3C). The dCas9 epi-suppressors and gRNAs were co-transfected into 293T cells. Using qPCR and western blotting, we found that endogenous *GRN* was significantly decreased by this epigenetic system, with a potency order of KRAB > EZH2 > DNMT3a (Figures 2F and 2G), similar to that seen in the pCMV-luciferase/copGFP reporter systems. Therefore, we focused on the dCas9-KRAB epigenetic system in this study.

We then tested this system in the Hep3B hepatoma cell line, with the focus on the dCas9-KRAB construct. Using qPCR, we demonstrated that this dCas9-KRAB epigenetic approach significantly inhibited the expression of *GRN* in Hep3B tumor cells as compared with the random gRNA (gCT) and dCas9 controls (Figure 2H). Western blotting also confirmed the epigenetic knockdown of *GRN* oncoprotein in Hep3B cells (Figure 2I). Taken together, these data demonstrate that it is feasible to harness this epigenetic approach to knock down *GRN* in hepatoma cells.

Epigenetic Silencing of GRN Is Associated with *De Novo* DNA Methylation

To delineate the mechanisms that silence *GRN* epigenetically, we first examined DNA methylation in the promoter of *GRN* (Figure 3A). In both dCas9 control (no epi-suppressor) and random gRNA (gCT) control groups, the *GRN* promoter was minimally methylated, in parallel with the abundant expression of *GRN* in Hep3B cells. However, epigenetic targeting by dCas9-KRAB induced *de novo* DNA methylation in the *GRN* promoter (Figures 3B and 3C), resulting in the silencing of *GRN* in tumor cells. Similarly, this induced DNA methylation was also observed with dCas9-DNMT3a and dCas9-KRAB treatments in 293T cells (Figure 3D). The TCGA data also showed a negative correlation between the status of DNA methylation in the *GRN* promoter (cg24420717) and *GRN* mRNA abundance in patients with hepatoma (Figure S4; Spearman correlation coefficient −0.29, p = 1.30E−08).

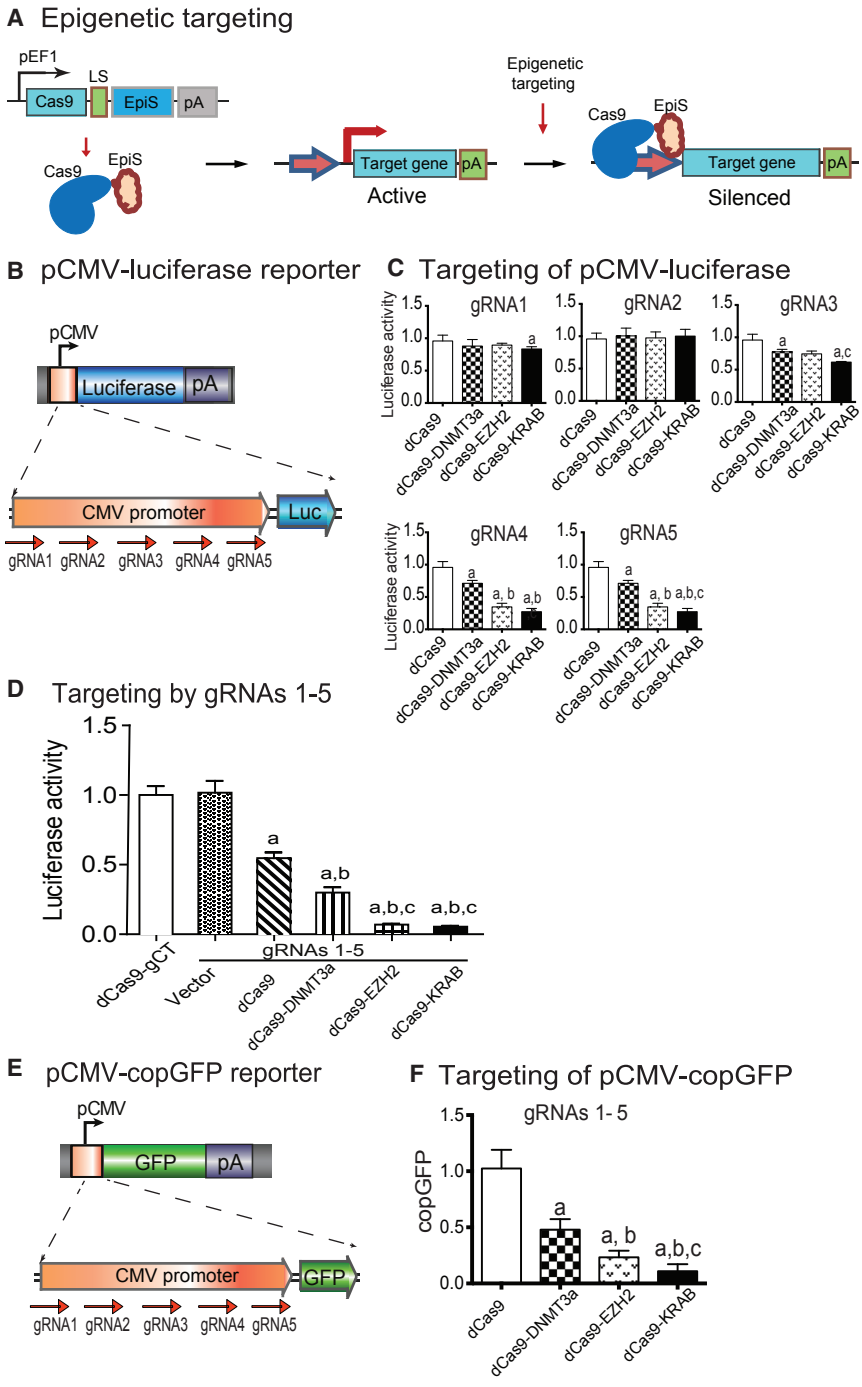

Figure 1. Gene Targeting by Synthetic dCas9 Epigenetic Suppressors

(A) Gene silencing by dCas9 epigenetic suppressors. pEF1, EF-1a promoters; LS, linker sequence; EpiS, epigenetic suppressors; pA, SV 40 poly(A) signal. Epigenetic suppressors are linked to the C-terminal of dCas9. With the aid of gRNA, dCas9 binds to the promoter or target genes, where the suppressors alter the promoter epigenotype and induce gene silencing. (B) The dCas9-luciferase reporter system. Luc, luciferase reporter gene; pCMV, CMV promoter; gRNA, guide RNAs used to target the CMV promoter that drives the luciferase reporter; PA, SV40 poly(A) signal. Arrows indicate the orientation of five gRNAs. (C) Epigenetic inhibition of the pCMV-luciferase. Epigenetic suppressor vectors, luciferase reporter vector, and pRL-TK control vector were co-transfected into cells with each gRNA or mixed gRNAs 1–5. At 48 hr after transfection, cells were collected for luciferase assay. All data shown are mean ± SD. a–c, $p < 0.05$ between the control and treatment groups. (D) Targeting of the pCMV-luciferase reporter by gRNA 1–5 mixture. Epigenetic suppressor and gRNA 1–5 vectors were co-transfected with pCMV-luciferase. gCT, scramble gRNA control; vector, the empty cloning vector and *GRN* gRNAs. All data shown are mean ± SD. a, $p < 0.05$ as compared with the scramble gRNA (gCT)-dCas9 and the gRNA-control vector (vector) group; b, $p < 0.05$ as compared with the dCas9 + gRNA group; c, $p < 0.05$ as compared with the dCas9-DNMT3a group. (E) The dCas9-copGFP reporter system. Arrows indicate the orientation of the gRNA. Inhibition of copGFP expression is shown. (F) Epigenetic inhibition of the pCMV-copGFP. The GFP fluorescence was measured 48 hr following transfection. All data shown are mean ± SD. a–c, $p < 0.05$ between the control and treatment groups.

Histone Modifications as Epigenetic Mechanisms for the Suppression of GRN

We then used a chromatin immunoprecipitation (ChIP) assay to examine the promoter histone code in the *GRN* promoter. We focused on histone H3 methylation at lysines 4, 9, and 27 (H3K4, H3K9, and H3K27). H3K4 is associated with an active promoter. We found that the treatment with dCas9-KRAB-gRNAs significantly reduced H3K4 methylation compared with three control groups (Figure 4A).

Methylation of H3K9 and H3K27 are suppressive markers on gene promoters. Transfection of cells with the dCas9-KRAB construct enhanced the H3K9 suppression signals in the *GRN* promoter (Figure 4B). However, no significant difference was noticed in H3K27 methylation as compared with the controls (Figure 4C).

Heterochromatin protein 1 (HP1a) functions as an epigenetic gatekeeper to inhibit gene activity by binding to H3K9 methylation marks. We found that dCas9-KRAB also induced a significant increment in HP1a binding to the *GRN* promoter, in parallel with increased H3K9 methylation and gene silencing (Figure 4D).

We also compared histone modifications induced by each dCas9 epi-suppressor treatment (Figure 4E). As compared with the dCas9-gRNA control, dCas9-EZH2 altered H3K4, H3K9, and H3K27. However, dCas9-DNMT3a did not significantly affect

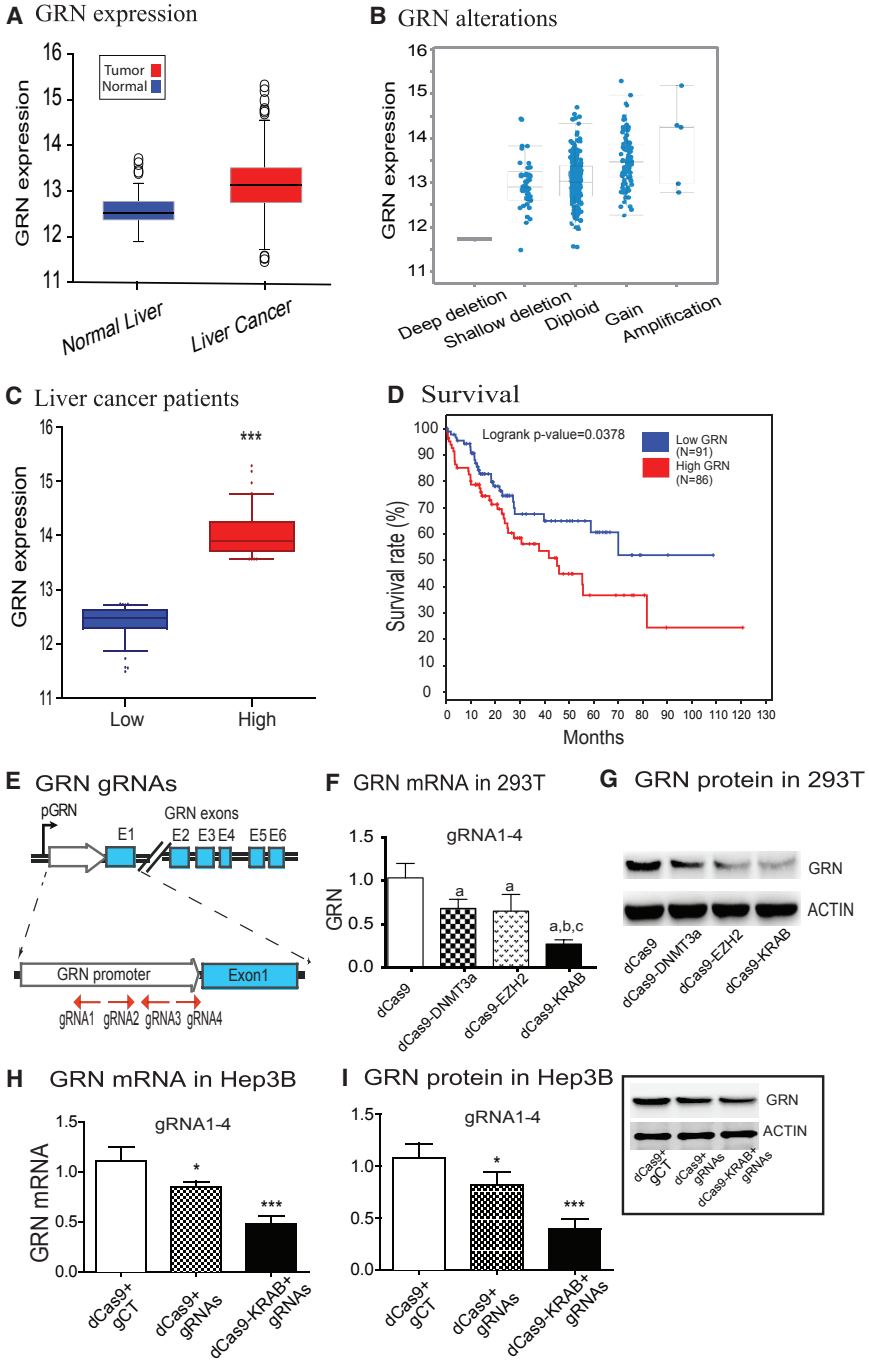

Figure 2. Epigenetic Inhibition of *GRN* by dCas9 Epigenetic Suppressors

(A) Upregulation of *GRN* in hepatoma. Differential expression of *GRN* was calculated from the mRNA-seq data of archived cancer and normal tissues in TCGA database. (B) Overexpression of *GRN* in hepatoma with genetic mutations. (C) Classification of the high and the low *GRN* expression in patients with hepatoma. (D) Low cancer survival in patients with high expression of *GRN*. The high (24%, n = 86) and the low (25%, n = 91) are shown. (E) Location of dCas9 gRNAs in the *GRN* promoter. Four *GRN* gRNAs were used to guide the epigenetic suppressors. p*GRN*, *GRN* promoter; E1–E6, *GRN* exons. (F) Inhibition of *GRN* mRNA in 293T cells. Cells were co-transfected with dCas9 epigenetic suppressors and *GRN* gRNAs 1–4. After transfection, cells were collected for the quantitation of *GRN* mRNA by RT-PCR. dCas9, cells treated with dCas9 plus *GRN* gRNAs 1–4. a–c, $p < 0.05$ between the control and treatment groups. (G) Western blot quantitation of *GRN* protein in 293T cells. β-ACTIN was used as the control. dCas9, cells treated with dCas9 plus *GRN* gRNAs 1–4. (H) Epigenetic inhibition of *GRN* in Hep3B hepatoma cells. Expression of *GRN* was quantitated by qPCR. dCas9-gCT, control cells treated with Cas9 plus *GRN* gRNAs 1–4. All data shown are mean ± SD. ***$p < 0.01$ as compared with the control group. (I) Western blot of *GRN*. Western blot image is shown in the window box. All data shown are mean ± SD. ***$p < 0.01$ as compared with the control group.

histone modifications in the *GRN* promoter. Interestingly, dCas9-KRAB not only altered histone modifications but also recruited HP1a to induce heterochromatin structure.

Epigenetic Targeting of GRN Reduces the Growth of Hep3B Hepatoma Cells

GRN is a cancer stem cell marker and plays an important role in regulating self-renewal of cancer stem cells. We examined if epigenetic silencing of *GRN* would affect the growth of tumor cells. We first examined cell proliferation using Hep3B cells. After epigenetic knockdown of *GRN*, there was a decrease in cell growth in the *GRN*-knocked down tumor cells as compared with the random gRNA control (gCT) and dCas9 control groups (Figure 5A).

We also examined if epigenetic knockdown of *GRN* altered the formation of tumor spheres (Figure 5B). After transfection with the dCas9-KRAB, Hep3B tumor cells were cultured in stem cell culture medium for 1 week. As expected, both the dCas9 control and random gRNA control cells formed clone spheres with compact structure. However, after knockdown of the cancer stem cell marker *GRN* with dCas9-KRAB, Hep3B cells exhibited a significant reduction in tumor spheres under the same culturing conditions.

We then tested the activity of the dCas9-KRAB treatment in altering cell invasion. Transwell was coated with Matrigel, a solubilized basement membrane preparation derived from the Engelbreth-Holm-Swarm mouse sarcoma. After epigenetic treatment, Hep3B cells were seeded on a Matrigel-coated transwell chamber,

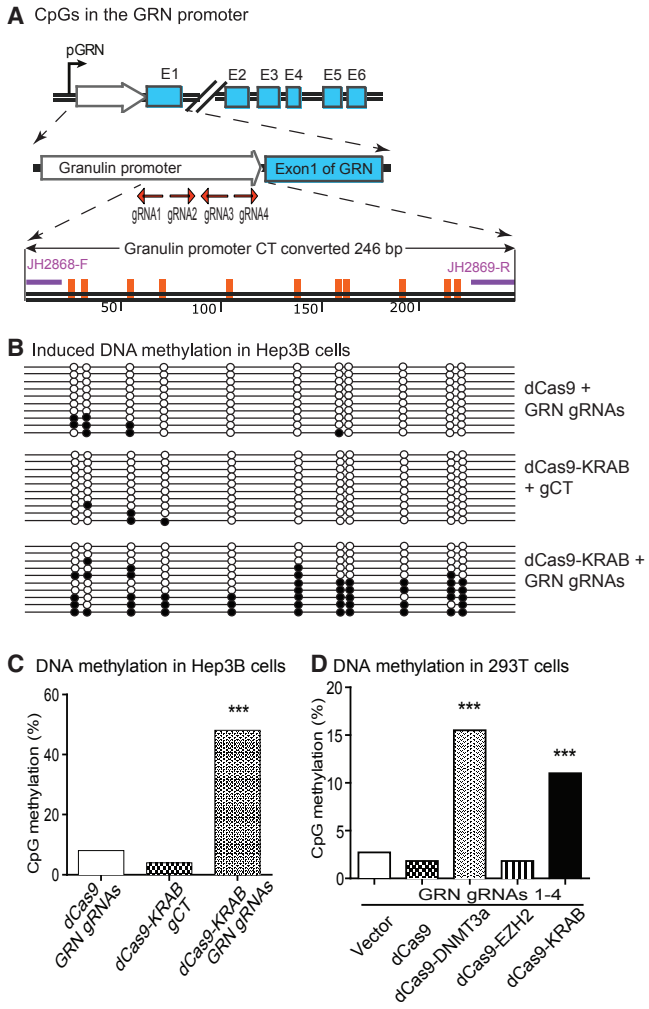

Figure 3. Induction of *De Novo* DNA Methylation in the *GRN* Promoter

(A) Location of gRNAs and CpG islands in the *GRN* promoter. (B) CpG DNA methylation of the *GRN* promoter in Hep3B stable cell clones. Black dots, methylated CpG sites; white dots, unmethylated CpG sites. Genomic DNA was treated with sodium bisulfate to convert unmethylated cytosines to uracils. The unmethylated and methylated DNAs were amplified by PCR and cloned into the pJet vector. Ten clones were randomly picked up from each group for quantitation of DNA methylation. (C) Quantitation of CpG methylation in Hep3B tumor cell clones. ***$p < 0.01$ as compared with the control group. (D) DNA methylation in transiently transfected 293T cells. Vector, cells treated with *GRN* gRNAs 1–4; dCas9, dCas9 plus *GRN* gRNAs 1–4. Cells were co-transfected with dCas9 and gRNA plasmid DNAs. After transient transfection, cells were collated and genomic DNAs were isolated for sodium bisulfate sequencing. We randomly picked up 10 clones in each treatment group for DNA sequencing. ***$p < 0.01$ as compared with the control groups.

and the number of cells that passed through the Matrigel to the bottom of the transwell was quantified as a measure of cell invasion. We found that, after treatment with dCas9 control and gCT control, Hep3B cells still exhibited the malignant phenotype of invading across the Matrigel membrane. However, epigenetic knockdown of *GRN* by dCas9-KRAB resulted in significantly lower invasion activity (Figure 5C; $p < 0.01$).

GRN Epigenetic Targeting Inhibits Hepatoma Cells through the TIMP/MMP Pathway

The TIMP/MMP pathway plays a critical role in cell migration and tumor metastasis. We investigated whether epigenetic knockdown of *GRN* affected the invasion of hepatoma cells through this pathway. As compared with the gCT non-targeting control, knockdown of *GRN* with dCas9-gRNAs significantly downregulated all the MMP family genes tested, including *MMP-7*, *MMP-9*, *MMP-11*, and *MMP14* (Figure 6A; $p < 0.01$). Among the TIMP family genes examined, both *TIMP1* and *TIMP2* were significantly upregulated after epigenetic knockdown of *GRN*. *TIMP3*, however, was slightly downregulated. *TIMP4* was not affected by this epigenetic targeting (Figure 6B). The TCGA data also showed the co-expression pattern of *GRN* with the TIMP/MMP family genes (Figure S5).

DISCUSSION

The CRISPR-associated nuclease Cas9 provides an effective means of introducing targeted loss of function at specific sites in the genome, raising the hope for therapeutic genome editing. By combining with co-expressed gRNAs, the nuclear-tagged Cas9 leads to the assembly of a specific endonuclease complex that can target any chromosomal DNA sequence for cleavage at a site immediately 5′ to an NGG PAM site. In this study, we show that, when linked with epigenetic suppressors DNMT3a, EZH2, and KRAB, the catalytically inactive dCas9 is able to introduce suppressive epigenetic marks into the promoter of a target gene.

The hepatic cancer stem cell marker *GRN* is located at 17q21.32, a region frequently involved in chromosome gain in liver cancers. *GRN* contributes to human cancers by potentiating neoplastic transformation, tumor growth, metastases, tissue invasion, and therapeutic resistance. The *GRN* promoter has been characterized in several cell lines, including A549 (lung carcinoma), CaSki (cervical carcinoma), NIH 3T3 (mouse fibroblast), and COS-7 cells (monkey kidney fibroblast).[26] It lacks a conventional TATA box, but it contains several potential CCAAT boxes and GC box elements. Mutations in the *GRN* gene result in autosomal dominant frontotemporal lobar degeneration (FTLD) associated with personality changes and progressive dementia.[30,31] In addition, the promoter activity is associated with epigenetic mutations, including increased DNA methylation in patients with sporadic FTLD[27,28] and altered histone acetylation.[29]

In this study, we utilized synthetic dCas9 epi-suppressors to epigenetically suppress *GRN* as a potential intervention for hepatoma. To precisely target the *GRN* promoter, we synthesized three dCas9 epigenetic constructs by tethering the C terminus of dCas9 to three suppressor domains derived from DNMT3a, EZH2, and KRAB. The synthetic suppressor factors contain a dCas9 DNA-binding domain that specifically binds to its *GRN* gene target under the guidance of gRNAs. The regulatory domain suppresses the promoter activity of *GRN* using an epigenetic mechanism. We demonstrate that all three

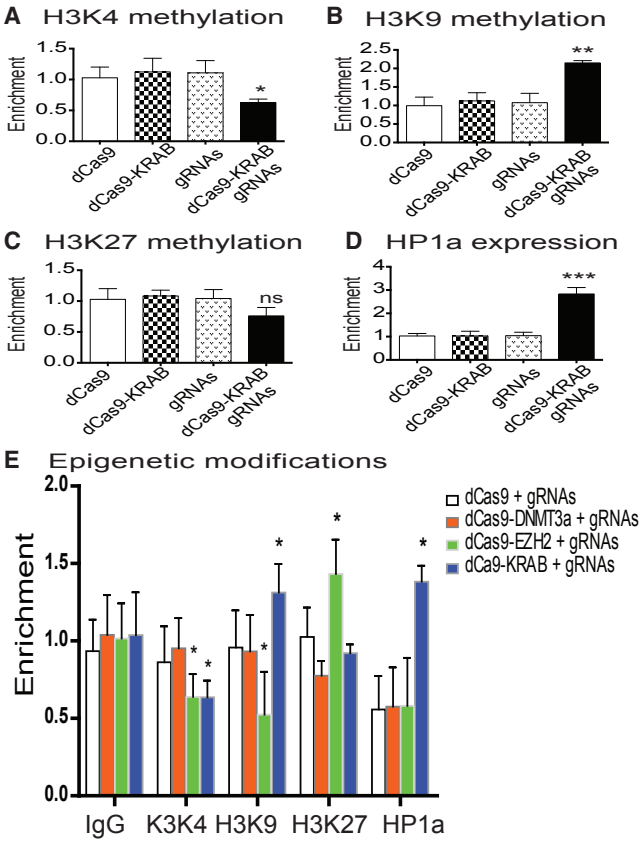

Figure 4. Histone Modifications and Heterochromatin Factor HP1a Binding in the *GRN* Promoter

(A–D) Histone modifications in cells treated with dCas9-KRAB construct. Epigenetic modifications in the *GRN* promoter were quantitated by ChIP using antibodies against trimethyl-H3K4 (A), trimethyl-H3K9 (B), trimethyl-H3K27 (C), and heterochromatin factor HP1 (D). *$p < 0.05$ as compared with the dCas9 control vector; **$p < 0.01$ as compared with dCas9 control vector; ***$p < 0.001$ as compared with dCas9 control vector; ns, non-statistical significance. (E) Histone modifications in cells treated with dCas9-epi-suppressor constructs. dCas9-gRNAs, cell controls that were treated with dCas9 plus *GRN* gRNAs 1–4; IgG, ChIP assay control that was immunoprecipitated by anti-IgG antibody. *$p < 0.05$ as compared with the dCas9 control vector. All data shown are mean ± SD.

synthetic epigenetic suppressors (dCas9-DNMT3a, dCas9-EZH2, and dCas9-KRAB) induce significant inhibition of *GRN* in Hep3B tumor cells. Using sodium bisulfite sequencing and ChIP, we show that dCas9 epigenetic targeting is associated with the induction of both *de novo* CpG DNA methylation and suppressive histone codes in the *GRN* promoter. Epigenetic targeting of *GRN* inhibited cell proliferation, tumor sphere formation, and cell invasion in Hep3B cells through the MMP/TIMP pathway. Thus, the synthetic dCas9 epi-suppressors may provide a powerful tool to epigenetically target *GRN* in tumor cells.

The suppressor domain of the synthetic dCas9 constructs can inhibit the target gene through several distinct epigenetic pathways, including histone modifications (H3K4, H3K9, and H3K27 lysine methylation), DNA methylation, and alteration of local chromatin structure.[32] DNA methylation-dependent repression is well established, especially for a CpG island-rich promoter. DNMT3a is a *de novo* DNA methyltransferase that methylates the C5 position of all cytosine nucleotides having the dinucleotide sequence 5′-CpG-3′. Once tethered to a target site, the enzyme methylates CpG islands in DNA sequences near the region where it binds. In this study, we demonstrate that the dCas9-DNMT3a is able to silence the CMV promoter in both luciferase and copGFP reporter systems.

Histone H3K9 or H3K27 methylation is normally associated with chromatin compaction and transcriptional silencing.[33–35] The H3K27 methyltransferase EZH2 relies on polycomb repressive complex 2 (PRC2) partners to achieve optimal activity.[36,37] In this study, we showed that, when tethered to the C terminus of dCas9, the EZH2 catalytic domain effectively inhibits the target promoters in 293T cells.

It is interesting to note that dCas9 epi-suppressors, like dCas9-KRAB, are able to use overlapping epigenetic pathways to suppress their target promoters. It is known that KRAB, the Krüppel-associated box, is present in the transcriptional repression domains of hundreds of human zinc-finger transcription factors.[38] KRAB functions as a transcriptional repressor to scaffold a silencing complex consisting of histone methyltransferase, the nucleosome remodeling and deacetylation (NuRD) complex, heterochromatin protein 1 (HP1), and DNA methyltransferases.[39,40] It can be directed to assemble multiprotein repression complexes on its target promoter.[41] In this study, we demonstrate that, after tethering to the *GRN* promoter, dCas9-KRAB was the most potent inhibitor in our system. It inhibits the expression of *GRN* in Hep3B tumor cells not only by introducing *de novo* DNA methylation but also by altering histone marks in the promoter, including decreased H3K4 methylation and enhanced H3K9 methylation. In addition, it recruits the heterochromatin protein HP1a. HP1 proteins are gatekeepers of epigenetic gene silencing. Working together, the synthetic dCas9-KRAB induces a substantial knockdown of the oncogenic *GRN* in hepatoma cells.

In summary, our data demonstrate that three epigenetic suppressors (DNMT3a, EZH2, and KRAB), when tethered to the gene promoter through the gRNA-guided dCas9, significantly inhibit the expression of target genes using distinct epigenetic mechanisms. dCas9-KRAB inhibits the target gene by multiple mechanisms, including *de novo* DNA methylation, H3K9 hypermethylation, and the recruitment of HP1a. Epigenetic silencing of *GRN* reduces invasion and tumor sphere formation in Hep3B tumor cells via the MMP/TIMP pathway. Our data demonstrate that this dCas9 epi-suppressor system may serve as a powerful epigenetic approach to inhibit therapeutic target genes in cancer cells.

MATERIALS AND METHODS

Cell Lines and Cell Culture

Hep3B (ATCC HB-8064) was purchased from ATCC and cultured in RP1640 medium supplemented with 10% fetal bovine serum (FBS)

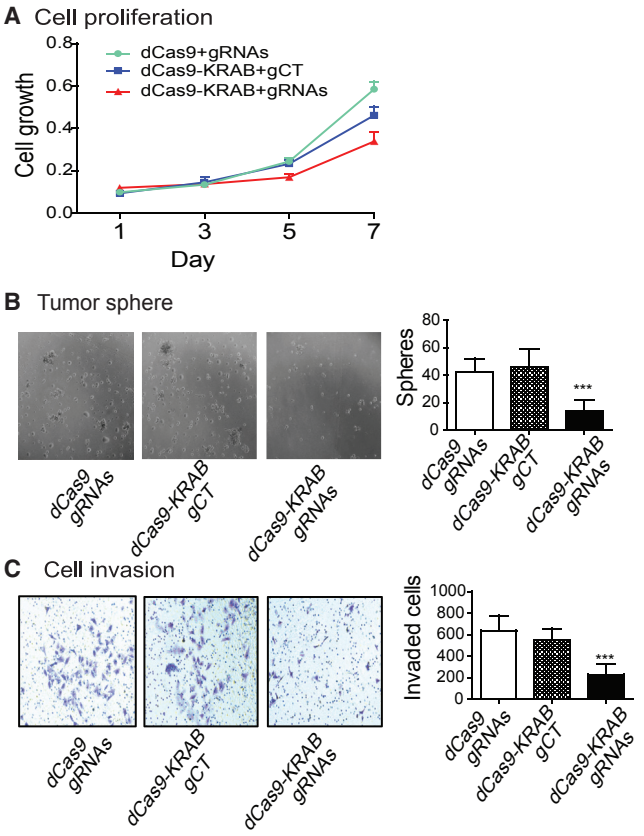

Figure 5. *GRN* Knockdown Suppresses Cell Proliferation, Invasion, and Tumor Sphere Formation

(A) Cell proliferation in Hep3B tumor cells after epigenetic silencing of *GRN*. (B) Tumor sphere formation in Hep3B cells following *GRN* suppression. (C) Reduced invasion of Hep3B cells by epigenetic inhibition of *GRN*. ***$p < 0.001$ as compared with dCas9 control vector. All data shown are mean ± SD.

and 100 U/mL penicillin-streptomycin. 293T cells were purchased from ATCC and cultured in DMEM (Invitrogen, CA) supplemented with 10% FBS (Invitrogen, CA), 1× Non-Essential Amino Acid (NEAA, Invitrogen, CA), and 100 U/mL penicillin-streptomycin (Invitrogen, CA). Cells were incubated at 37°C in 5% CO_2 air atmosphere.

Construction of the dCas9 Epi-suppressors

The CRISPR dCas9 plasmid was purchased from Addgene as a gift from Prashant Mali.[42] The humanized KRAB domain was synthesized from human cDNAs by overlapping PCR and verified by DNA sequence.[32] The full-length cDNA of DNMT3a (MHS6278-202759692) and EZH2 (MHS6278-202756846) were purchased from GE (Dharmacon, CO), and they were used for PCR cloning. The catalytically inactive dCas9 was created by D10A and H840A point mutation with Q5 Site-Directed Mutagenesis Kit (New England Biolabs, MA) and cloned into pCDH1 plasmid (SBI, CA).[43] Three epigenetic suppressors, KRAB, EZH2, and DNMT3 (DNMT3a catalytic domain C-terminal),[44,45] were amplified by PCR, and they were ligated into the C terminus of the dCas9 sequence in the pCDH1 vector, respectively, to obtain dCas9-KRAB, dCas9-EZH2, and dCas9-DNMT3a vector constructs. gRNAs that target the *GRN* promoter were cloned into pGreenPuro (SBI, CA).

Plasmid Transfection

Plasmids were transfected into target cell lines (293T and Hep3B) using Lipofectamine 2000 (Invitrogen, CA), following the protocol provided by the manufacturer. Briefly, cells were seeded in a 6-well plate at 4×10^5/well. After overnight culture, 4 μg constructed plasmids and 10 μL Lipofectamine 2000 were mixed in 250 μL Opti-Media (Opti-MEM I Reduced Serum Medium) (Gibco, CA). After incubation for 5 min at room temperature, the DNA-Lipofetamine 2000 mixture was added to target cells, and the culture medium was replaced with fresh medium 6 hr following transfection.

For the lentivirus package, the dCas9 epi-suppressor plasmids were co-transfected with pSPAX2 and pMD2.G packaging vectors in 293T cells using Lipofectamine 2000. The supernatants containing the lentiviruses were collected at 48 and 72 hr after transfection for cell study.[46,47]

Lentivirus Transduction

293T and Hep3B cells were seeded on 6-well plates. When cells reached 70%–90% confluency, 0.5 mL viral supernatant (MOI of 20) and 1 μL polybrene (10 mg/mL) were mixed in 1.5 mL DMEM and added onto the cell layer. After 24 hr, cells were cultured with normal media for 2–3 days. Puromycin was used to select stable clones.

Gene Activity by Luciferase Assay

Fresh 293T cells were seeded into 48-well plates at a density of 1×10^5 cells per well. The dCas9 epi-suppressor vectors, luciferase reporter vector, and pRL-TK control vector were co-transfected into cells using Lipofectamine 2000 (Invitrogen, CA). Cell lysates were harvested 48 hr after transfection, and dual-luciferase reporter assays were performed using a Turner Biosystems Single Tube Luminometer (Promega, WI).[32]

Quantitation of GFP Fluorescence by Luminometer

293T cells were seeded in 12-well plates at a density of 3×10^5 cells per well. The dCas9 epi-suppressor vectors and GFP reporter vector were co-transfected into 293T cells. At 48 hr after transfection, lysates were harvested and GFP expression assays were performed using a Turner Biosystems Single Tube Luminometer (Promega, WI).

Promoter Histone Suppression Code by ChIP

ChIP assays for histone methylation and HP1a recruitment were performed using an EZ-Magna ChIP G Kit (Millipore, CA). Briefly, monoclonal Hep3B cells with stable expression of copGFP in 10-cm dishes were transiently transfected with 15 μg suppressor vectors. At 48 hr after transfection, cells were cross-linked with

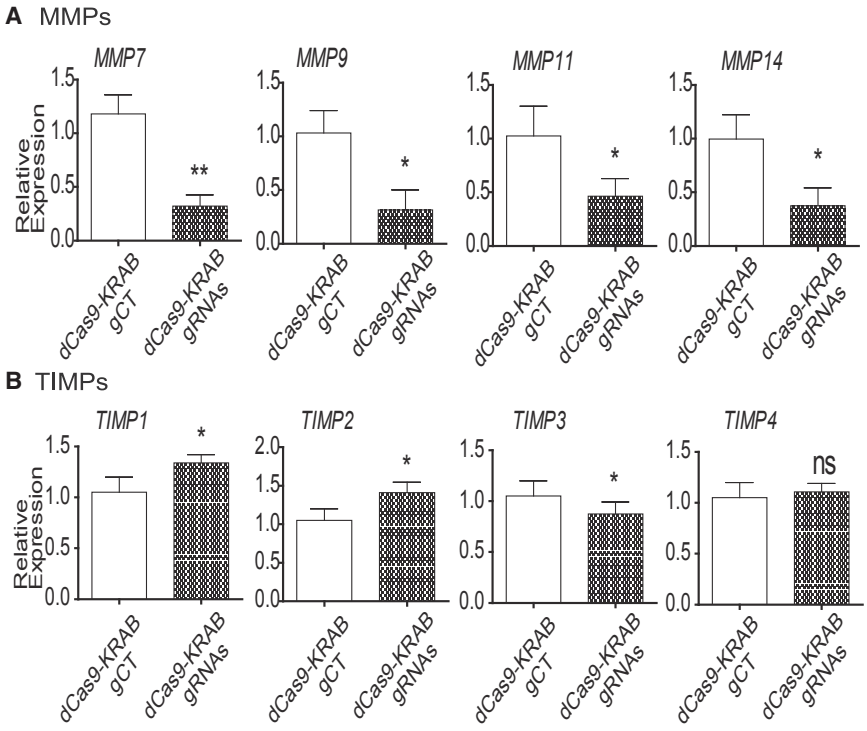

Figure 6. Mechanisms Underlying Epigenetic Suppressor-Induced Inhibition of Cell Proliferation, Invasion, and Tumor Sphere

(A) Inhibition of the MMP family genes. Expression of the MMP family genes was quantitated by qPCR in Hep3B cells. (B) Alteration of the TIMP family genes. Expression of the TIMP family genes was measured by qPCR. *$p < 0.01$ as compared with dCas9 control vector; **$p < 0.001$ as compared with dCas9 control vector; ns, non-statistical significance. All data shown are mean ± SD.

1% formaldehyde (Sigma, MO) and harvested for immunoprecipitation. Antibodies used in ChIP assays included anti-H4K4Me3, anti-H3K9Me3, anti-H3K27Me3, and anti-HP1a (Millipore, CA).[32] An aliquot of cell lysates was saved to serve as the input DNA control. After the reversal of cross-linking at 62°C for 2 hr and 95°C for 10 min, ChIP samples were purified and subjected to real-time qPCR. Individual ChIP assays were repeated three times to confirm the reproducibility of the qPCR. Real-time qPCR was performed using 2xKapa mixed with SYBR (Applied Biosystems, CA) on an ABI PRISM 7900 HT Sequence Detection System (Applied Biosystems, CA) with *GRN* primers (forward, 5′-GCGGTTTTGGCAGTACATCA-3′; reverse, 5′-GGGCGGAGTTGTTACGACAT-3′). Individual ChIP assays were repeated three times to confirm the reproducibility of the qPCR.

DNA Methylation by Bisulfate Sequencing

Transiently transfected 293T and stably transducted monoclonal Hep3B cells with dCas9-KRAB were selected by puromycin. Stable cells (1×10^6) were collected and genomic DNA was extracted. Genomic DNAs were converted by bisulfite sodium using an EZ DNA MethylationGold kit (Zymo Research, CA) and purified using a DNA purification kit (QIAGEN, CA). DNA samples were amplified with PCR primers JH1369F: 5′-GGAGGTAGAGGTTGTAGT GAG-3′and JH1370R: 5′-AACAACCTCAACAAAACAACTAA TAC-3′ that cover 11 CpG islands in the *GRN* promoter. After 2% agarose gel electrophoresis, the predicted bands (240 bp) of the PCR product were recovered using a gel purification kit (QIAGEN, CA), cloned into the pJet vector, and sequenced for the quantitation of CpG methylation. DNA methylation was calculated as the average percentage of all CpG sites.

Cell Proliferation by MTT Assay

Cell survival was measured using the (3-(4,5-dimethylthiazol-2-yl)-2,5-diphenyltetrazolium bromide) tetrazolium (MTT) assay.[48,49] Briefly, cells (1×10^4/well) were plated onto 96-well plates, and they were incubated with 20 μL 5 mg/mL MTT (Sigma, MO) per well at 37°C for 4 hr. The absorbance was measured at 490 nm using a microplate reader (BioTek Instruments). Cell viability (%) was calculated based on the following equation: cell viability (%)1/4(Asample/Acontrol) × 100%, where Asample and Acontrol represent the absorbance of the sample and control wells, respectively.

Western Blot Analysis

Western blot was used to detect the secreted *GRN* proteins in cell supernatants. Briefly, 293T cells were transfected with dCas9-KRAB + scramble gRNA plasmids for control group and dCas9-KRAB + *GRN* gRNA plasmids for treatment group. At 48 hr after transfection, cell supernatants (20 μL) were separated on Mini-PROTEIN TGX gradient gel (Bio-Rad, CA) and transferred to a nitrocellulose membrane. After blocking with Odyssey Blocking buffer for 1 hr, membranes were incubated with specific primary antibodies against GRN (Abcam, ab55167) and Anti-beta Actin antibody (Abcam, ab8227) overnight at 4°C. After washing with PBS 4 times, the IRDye 680 secondary antibody (LI-COR Biosciences, Lincoln, NE) was added and the infrared fluorescence was visualized with the Odyssey infrared imaging system (LI-COR Biosciences, Lincoln, NE).[50]

Cell Invasion by Transwell Assay

In the invasion assay, cells were seeded on the upper chamber (4×10^5 cells per well) of six-well Transwell plates equipped with polycarbonate filters coated with 1.0 mL 1:8 diluted Matrigel (300 μg/mL/well) (BD Biosciences, CA, 356231) in serum-free medium. DMEM with 5% FBS was added to the lower chamber as the chemoattractant. After 24 hr of incubation at 37°C, filters were cleaned on the upper side with a cotton swab, fixed with

100% methanol, and stained with 0.1% crystal violet. Crystal violet was washed from the cells using 4 mL 33% acetic acid. The absorbance of the washed liquid was determined at 590 nm. All samples were performed in triplicate.[51]

Real-Time qPCR

Genomic, bisulfate-converted DNA and mRNA were extracted using DNeasy Blood & Tissue Kit (QIAGEN, CA), EZ DNA MethylationGold kit (Zymo Research, CA), and RNeasy Mini Kit (QIAGEN, CA), and mRNAs were reverse-transcribed using M-MLV Reverse Transcriptase (Thermo Fisher Scientific, CA). Real-time qPCR was performed using 2xKapa mixed with SYBR (Applied Biosystems, CA) on an ABI PRISM 7900 HT Sequence Detection System (Applied Biosystems, CA) with primers. All experiments were performed in triplicate. PCR primers used for qPCR are listed in Table S1.

Sphere Formation Assay

Hep3B cells were seeded in serum-free medium (SFM), containing DMEM/F12 (Gibco, CA) supplemented with 20 ng/mL epidermal growth factor (EGF) (Invitrogen, CA), 10 ng/mL basic fibroblast growth factor (bFGF) (Invitrogen, CA), 5 μg/mL insulin (Invitrogen, CA), and 10 μL/mL B27 (Invitrogen, CA), at 1×10^4 cells/well in Sigmacote- (Sigma, MO) coated 6-well plates. Cells were then incubated at 37°C in a humidified atmosphere containing 5% CO_2. The spheres were counted on day 10; we counted 10 fields of spheres at 40× phase view for each group, and all samples were performed in triplicate.[52,53]

Acquisition of TCGA Data

Clinical data of *GRN* expression were generated from the TCGA Research Network (https://cancergenome.nih.gov). The liver hepatocellular carcinoma (LIHC) TCGA provisional RNA sequencing (RNA-seq) cohorts with 442 samples were used for calculation. Clinical annotation of samples was obtained from http://firebrowse.org/?cohort=LIHC. The differential expression of *GRN* between normal liver and liver cancer was generated by the Gene expression viewer of FIREBROWSE (http://firebrowse.org/viewGene.html?gene=GRN). The *GRN* putative copy number alterations plot, mRNA and methylation correlation plot, survival plot, *GRN* co-occurrence plot, and TIMP/MMP pathway gene co-expression plot were generated by cbioportal.[54,55] For the survival analysis, we grouped the patients into two groups based on *GRN* mRNA expression: the high *GRN* group (higher 24%) 86 cases and the low *GRN* group (25%) 91 cases. We used Mexpression[56] to analyze the correlation between *GRN* DNA methylation and mRNA expression, and we also referred to the pre-analyzed data from Broad Institute TCGA GDAC (http://gdac.broadinstitute.org/runs/analyses__2015_08_21/reports/cancer/LIHC-TP/Correlate_Methylation_vs_mRNA/nozzle.html).

Statistical Analysis

All experiments were performed in triplicate and the data were expressed as mean ± SD. The comparative *CT* method was applied in the real-time qRT-PCR assay according to the delta-delta *CT* method. Data were analyzed using SPSS software (version 20.0; SPSS, IL). One-way ANOVA (Bonferroni test) was used to compare statistical differences for variables among treatment groups. The data were considered statistically significant at $p < 0.05$.

SUPPLEMENTAL INFORMATION

Supplemental Information includes five figures and three tables and can be found with this article online at https://doi.org/10.1016/j.omtn.2018.01.002.

AUTHOR CONTRIBUTIONS

J.-F.H., J.C., W.L., and A.R.H. conceived and designed the experiment, H.W., R.G., Z.D., L.B., and L.L. performed the experiments; H.W. and R.G. analyzed data; J.-F.H. and H.W. wrote the paper.

CONFLICTS OF INTEREST

No conflicts of interest were disclosed.

ACKNOWLEDGMENTS

This work was supported by the National Natural Science Foundation of China grants (31430021 and 81272294), the National Basic Research Program of China (973 Program) (2015CB943303), and California Institute of Regenerative Medicine (CIRM) grant (RT2-01942) to J.-F.H.; the National Natural Science Foundation of China grant (81500116) to H.W.; the National Natural Science Foundation of China grant (81601449) to R.G.; by Key Project of Chinese Ministry of Education grant (311015), National Natural Science Foundation of China grant (81672275), Nation Key Research and Development Program of China grant (2016YFC13038000), Natural Science Foundation of Jilin Province grant (20150101176JC), Research on Chronic Noncommunicable Diseases Prevention and Control of National Ministry of Science and Technology (2016YFC1303804), and National Health Development Planning Commission Major Disease Prevention and Control of Science and Technology Plan of Action, Cancer Prevention and Control (ZX-07-C2016004) to J.C.; the National Natural Science Foundation of China grants (81372835 and 81670143) and Jilin Science and Technique International Collaboration grant (20130413010GH) to W.L.; and the Department of Veterans Affairs Research Service.

REFERENCES

1. Ferlay, J., Soerjomataram, I., Dikshit, R., Eser, S., Mathers, C., Rebelo, M., Parkin, D.M., Forman, D., and Bray, F. (2015). Cancer incidence and mortality worldwide: sources, methods and major patterns in GLOBOCAN 2012. Int. J. Cancer *136*, E359–E386.

2. Torre, L.A., Bray, F., Siegel, R.L., Ferlay, J., Lortet-Tieulent, J., and Jemal, A. (2015). Global cancer statistics, 2012. CA Cancer J. Clin. *65*, 87–108.

3. Best, J., Schotten, C., Theysohn, J.M., Wetter, A., Müller, S., Radünz, S., Schulze, M., Canbay, A., Dechêne, A., and Gerken, G. (2017). Novel implications in the treatment of hepatocellular carcinoma. Ann. Gastroenterol. *30*, 23–32.

4. Bakhtiar, A., Sayyad, M., Rosli, R., Maruyama, A., and Chowdhury, E.H. (2014). Intracellular delivery of potential therapeutic genes: prospects in cancer gene therapy. Curr. Gene Ther. *14*, 247–257.

5. Yeh, J.E., Kreimer, S., Walker, S.R., Emori, M.M., Krystal, H., Richardson, A., Ivanov, A.R., and Frank, D.A. (2015). Granulin, a novel STAT3-interacting protein, enhances STAT3 transcriptional function and correlates with poorer prognosis in breast cancer. Genes Cancer *6*, 153–168.

6. Cheung, P.F., Cheung, T.T., Yip, C.W., Ng, L.W., Fung, S.W., Lo, C.M., Fan, S.T., and Cheung, S.T. (2016). Hepatic cancer stem cell marker granulin-epithelin precursor and β-catenin expression associate with recurrence in hepatocellular carcinoma. Oncotarget *7*, 21644–21657.
7. Yip, C.W., Cheung, P.F., Leung, I.C., Wong, N.C., Cheng, C.K., Fan, S.T., and Cheung, S.T. (2014). Granulin-epithelin precursor interacts with heparan sulfate on liver cancer cells. Carcinogenesis *35*, 2485–2494.
8. Sato-Matsubara, M., and Kawada, N. (2017). New player in tumor-stromal interaction: Granulin as a novel therapeutic target for pancreatic ductal adenocarcinoma liver metastasis. Hepatology *65*, 374–376.
9. Singh, V., Braddick, D., and Dhar, P.K. (2017). Exploring the potential of genome editing CRISPR-Cas9 technology. Gene *599*, 1–18.
10. Stella, S., and Montoya, G. (2016). The genome editing revolution: A CRISPR-Cas TALE off-target story. BioEssays *38* (*Suppl 1*), S4–S13.
11. Tschaharganeh, D.F., Lowe, S.W., Garippa, R.J., and Livshits, G. (2016). Using CRISPR/Cas to study gene function and model disease in vivo. FEBS J. *283*, 3194–3203.
12. Wang, K., Tang, X., Liu, Y., Xie, Z., Zou, X., Li, M., Yuan, H., Ouyang, H., Jiao, H., and Pang, D. (2016). Efficient Generation of Orthologous Point Mutations in Pigs via CRISPR-assisted ssODN-mediated Homology-directed Repair. Mol. Ther. Nucleic Acids *5*, e396.
13. Wang, X., Huang, X., Fang, X., Zhang, Y., and Wang, W. (2016). CRISPR-Cas9 System as a Versatile Tool for Genome Engineering in Human Cells. Mol. Ther. Nucleic Acids *5*, e388.
14. Tycko, J., Myer, V.E., and Hsu, P.D. (2016). Methods for Optimizing CRISPR-Cas9 Genome Editing Specificity. Mol. Cell *63*, 355–370.
15. Osborn, M.J., Belanto, J.J., Tolar, J., and Voytas, D.F. (2016). Gene editing and its application for hematological diseases. Int. J. Hematol. *104*, 18–28.
16. Eid, A., and Mahfouz, M.M. (2016). Genome editing: the road of CRISPR/Cas9 from bench to clinic. Exp. Mol. Med. *48*, e265.
17. Fogleman, S., Santana, C., Bishop, C., Miller, A., and Capco, D.G. (2016). CRISPR/Cas9 and mitochondrial gene replacement therapy: promising techniques and ethical considerations. Am. J. Stem Cells *5*, 39–52.
18. Qi, L.S., Larson, M.H., Gilbert, L.A., Doudna, J.A., Weissman, J.S., Arkin, A.P., and Lim, W.A. (2013). Repurposing CRISPR as an RNA-guided platform for sequence-specific control of gene expression. Cell *152*, 1173–1183.
19. Gasiunas, G., Barrangou, R., Horvath, P., and Siksnys, V. (2012). Cas9-crRNA ribonucleoprotein complex mediates specific DNA cleavage for adaptive immunity in bacteria. Proc. Natl. Acad. Sci. USA *109*, E2579–E2586.
20. Sachdeva, M., Sachdeva, N., Pal, M., Gupta, N., Khan, I.A., Majumdar, M., and Tiwari, A. (2015). CRISPR/Cas9: molecular tool for gene therapy to target genome and epigenome in the treatment of lung cancer. Cancer Gene Ther. *22*, 509–517.
21. Gori, J.L., Hsu, P.D., Maeder, M.L., Shen, S., Welstead, G.G., and Bumcrot, D. (2015). Delivery and Specificity of CRISPR-Cas9 Genome Editing Technologies for Human Gene Therapy. Hum. Gene Ther. *26*, 443–451.
22. Pellagatti, A., Dolatshad, H., Valletta, S., and Boultwood, J. (2015). Application of CRISPR/Cas9 genome editing to the study and treatment of disease. Arch. Toxicol. *89*, 1023–1034.
23. Dominguez, A.A., Lim, W.A., and Qi, L.S. (2016). Beyond editing: repurposing CRISPR-Cas9 for precision genome regulation and interrogation. Nat. Rev. Mol. Cell Biol. *17*, 5–15.
24. Bono, J.M., Olesnicky, E.C., and Matzkin, L.M. (2015). Connecting genotypes, phenotypes and fitness: harnessing the power of CRISPR/Cas9 genome editing. Mol. Ecol. *24*, 3810–3822.
25. Mandegar, M.A., Huebsch, N., Frolov, E.B., Shin, E., Truong, A., Olvera, M.P., Chan, A.H., Miyaoka, Y., Holmes, K., Spencer, C.I., et al. (2016). CRISPR Interference Efficiently Induces Specific and Reversible Gene Silencing in Human iPSCs. Cell Stem Cell *18*, 541–553.
26. Bhandari, V., Daniel, R., Lim, P.S., and Bateman, A. (1996). Structural and functional analysis of a promoter of the human granulin/epithelin gene. Biochem. J. *319*, 441–447.
27. Galimberti, D., D'Addario, C., Dell'osso, B., Fenoglio, C., Marcone, A., Cerami, C., Cappa, S.F., Palazzo, M.C., Arosio, B., Mari, D., et al. (2013). Progranulin gene (*GRN*) promoter methylation is increased in patients with sporadic frontotemporal lobar degeneration. Neurol. Sci. *34*, 899–903.
28. Banzhaf-Strathmann, J., Claus, R., Mücke, O., Rentzsch, K., van der Zee, J., Engelborghs, S., De Deyn, P.P., Cruts, M., van Broeckhoven, C., Plass, C., and Edbauer, D. (2013). Promoter DNA methylation regulates progranulin expression and is altered in FTLD. Acta Neuropathol. Commun. *1*, 16.
29. She, A., Kurtser, I., Reis, S.A., Hennig, K., Lai, J., Lang, A., Zhao, W.N., Mazitschek, R., Dickerson, B.C., Herz, J., and Haggarty, S.J. (2017). Selectivity and Kinetic Requirements of HDAC Inhibitors as Progranulin Enhancers for Treating Frontotemporal Dementia. Cell Chem. Biol. *24*, 892–906.e5.
30. Curtis, A.F., Masellis, M., Hsiung, G.R., Moineddin, R., Zhang, K., Au, B., Millett, G., Mackenzie, I., Rogaeva, E., and Tierney, M.C. (2017). Sex differences in the prevalence of genetic mutations in FTD and ALS: A meta-analysis. Neurology *89*, 1633–1642.
31. Kumar-Singh, S. (2011). Progranulin and TDP-43: mechanistic links and future directions. J. Mol. Neurosci. *45*, 561–573.
32. Ma, A.N., Wang, H., Guo, R., Wang, Y.X., Li, W., Cui, J., Wang, G., Hoffman, A.R., and Hu, J.F. (2014). Targeted gene suppression by inducing de novo DNA methylation in the gene promoter. Epigenetics Chromatin *7*, 20.
33. Goyama, S., and Kitamura, T. (2017). Epigenetics in normal and malignant hematopoiesis: An overview and update 2017. Cancer Sci. *108*, 553–562.
34. Mozzetta, C., Pontis, J., and Ait-Si-Ali, S. (2015). Functional Crosstalk Between Lysine Methyltransferases on Histone Substrates: The Case of G9A/GLP and Polycomb Repressive Complex 2. Antioxid. Redox Signal. *22*, 1365–1381.
35. Nichol, J.N., Dupéré-Richer, D., Ezponda, T., Licht, J.D., and Miller, W.H., Jr. (2016). H3K27 Methylation: A Focal Point of Epigenetic Deregulation in Cancer. Adv. Cancer Res. *131*, 59–95.
36. Moritz, L.E., and Trievel, R.C. (2017). Structure, mechanism, and regulation of polycomb repressive complex 2. J. Biol. Chem. *September 14*, jbc.R117.800367.
37. Gall Trošelj, K., Novak Kujundzic, R., and Ugarkovic, D. (2016). Polycomb repressive complex's evolutionary conserved function: the role of EZH2 status and cellular background. Clin. Epigenetics *8*, 55.
38. Ecco, G., Imbeault, M., and Trono, D. (2017). KRAB zinc finger proteins. Development *144*, 2719–2729.
39. Yang, P., Wang, Y., and Macfarlan, T.S. (2017). The Role of KRAB-ZFPs in Transposable Element Repression and Mammalian Evolution. Trends Genet. *33*, 871–881.
40. Imbeault, M., Helleboid, P.Y., and Trono, D. (2017). KRAB zinc-finger proteins contribute to the evolution of gene regulatory networks. Nature *543*, 550–554.
41. Wolf, G., Greenberg, D., and Macfarlan, T.S. (2015). Spotting the enemy within: Targeted silencing of foreign DNA in mammalian genomes by the Krüppel-associated box zinc finger protein family. Mob. DNA *6*, 17.
42. Mali, P., Yang, L., Esvelt, K.M., Aach, J., Guell, M., DiCarlo, J.E., Norville, J.E., and Church, G.M. (2013). RNA-guided human genome engineering via Cas9. Science *339*, 823–826.
43. Zhang, Y., Hu, J.F., Wang, H., Cui, J., Gao, S., Hoffman, A.R., and Li, W. (2017). CRISPR Cas9-guided chromatin immunoprecipitation identifies miR483 as an epigenetic modulator of IGF2 imprinting in tumors. Oncotarget *8*, 34177–34190.
44. Rivenbark, A.G., Stolzenburg, S., Beltran, A.S., Yuan, X., Rots, M.G., Strahl, B.D., and Blancafort, P. (2012). Epigenetic reprogramming of cancer cells via targeted DNA methylation. Epigenetics *7*, 350–360.
45. Tatton-Brown, K., Seal, S., Ruark, E., Harmer, J., Ramsay, E., Del Vecchio Duarte, S., Zachariou, A., Hanks, S., O'Brien, E., Aksglaede, L., et al.; Childhood Overgrowth Consortium (2014). Mutations in the DNA methyltransferase gene DNMT3A cause an overgrowth syndrome with intellectual disability. Nat. Genet. *46*, 385–388.
46. Sun, J., Li, W., Sun, Y., Yu, D., Wen, X., Wang, H., Cui, J., Wang, G., Hoffman, A.R., and Hu, J.F. (2014). A novel antisense long noncoding RNA within the IGF1R gene locus is imprinted in hematopoietic malignancies. Nucleic Acids Res. *42*, 9588–9601.
47. Wang, H., Li, W., Guo, R., Sun, J., Cui, J., Wang, G., Hoffman, A.R., and Hu, J.F. (2014). An intragenic long noncoding RNA interacts epigenetically with the

RUNX1 promoter and enhancer chromatin DNA in hematopoietic malignancies. Int. J. Cancer *135*, 2783–2794.

48. Zhang, H., Zeitz, M.J., Wang, H., Niu, B., Ge, S., Li, W., Cui, J., Wang, G., Qian, G., Higgins, M.J., et al. (2014). Long noncoding RNA-mediated intrachromosomal interactions promote imprinting at the Kcnq1 locus. J. Cell Biol. *204*, 61–75.

49. Yin, H., Chen, N., Guo, R., Wang, H., Li, W., Wang, G., Cui, J., Jin, H., and Hu, J.F. (2015). Antitumor potential of a synthetic interferon-alpha/PLGF-2 positive charge peptide hybrid molecule in pancreatic cancer cells. Sci. Rep. *5*, 16975.

50. Zhang, S., Zhong, B., Chen, M., Yang, L., Yang, G., Li, Y., Wang, H., Wang, G., Li, W., Cui, J., et al. (2014). Epigenetic reprogramming reverses the malignant epigenotype of the MMP/TIMP axis genes in tumor cells. Int. J. Cancer *134*, 1583–1594.

51. Zhao, X., Liu, X., Wang, G., Wen, X., Zhang, X., Hoffman, A.R., Li, W., Hu, J.F., and Cui, J. (2016). Loss of insulin-like growth factor II imprinting is a hallmark associated with enhanced chemo/radiotherapy resistance in cancer stem cells. Oncotarget *7*, 51349–51364.

52. Song, W., Li, W., Li, L., Zhang, S., Yan, X., Wen, X., Zhang, X., Tian, H., Li, A., Hu, J.F., and Cui, J. (2015). Friend leukemia virus integration 1 activates the Rho GTPase pathway and is associated with metastasis in breast cancer. Oncotarget *6*, 23764–23775.

53. Uchida, Y., Tanaka, S., Aihara, A., Adikrisna, R., Yoshitake, K., Matsumura, S., Mitsunori, Y., Murakata, A., Noguchi, N., Irie, T., et al. (2010). Analogy between sphere forming ability and stemness of human hepatoma cells. Oncol. Rep. *24*, 1147–1151.

54. Gao, J., Aksoy, B.A., Dogrusoz, U., Dresdner, G., Gross, B., Sumer, S.O., Sun, Y., Jacobsen, A., Sinha, R., Larsson, E., et al. (2013). Integrative analysis of complex cancer genomics and clinical profiles using the cBioPortal. Sci. Signal. *6*, pl1.

55. Cerami, E., Gao, J., Dogrusoz, U., Gross, B.E., Sumer, S.O., Aksoy, B.A., Jacobsen, A., Byrne, C.J., Heuer, M.L., Larsson, E., et al. (2012). The cBio cancer genomics portal: an open platform for exploring multidimensional cancer genomics data. Cancer Discov. *2*, 401–404.

56. Koch, A., De Meyer, T., Jeschke, J., and Van Criekinge, W. (2015). MEXPRESS: visualizing expression, DNA methylation and clinical TCGA data. BMC Genomics *16*, 636.